PHYSICAL REVIEW B **78**, 121401(R) (2008)

Room-temperature superfluidity in graphene bilayers

Hongki Min, Rafi Bistritzer, Jung-Jung Su, and A. H. MacDonald
Department of Physics, The University of Texas at Austin, Austin Texas 78712, USA
(Received 6 July 2008; published 3 September 2008)

Because graphene is an atomically two-dimensional gapless semiconductor with nearly identical conduction and valence bands, graphene-based bilayers are attractive candidates for high-temperature electron-hole pair condensation. We present estimates which suggest that the Kosterlitz-Thouless temperatures of these two-dimensional counterflow superfluids can approach room temperature.

DOI: 10.1103/PhysRevB.78.121401 PACS number(s): 71.35.−y, 71.10.−w, 73.21.−b, 73.22.Gk

I. INTRODUCTION

Electron-hole pair (exciton) condensates were first proposed[1,2] as possible ordered states of solids more than forty years ago but have proved difficult to realize experimentally. Progress has been made recently with the discovery[3,4] of equilibrium exciton condensation below $T \sim 1$ K in the quantum Hall regime, the identification[5] of spontaneous coherence effects in cold optically excited exciton gases, and studies of dynamic condensation[6] of polaritons in nonresonantly pumped optical microcavities. In the weak-coupling limit, exciton condensation is a consequence of the Cooper instability[2] of solids with occupied conduction-band states and empty valence-band states inside identical Fermi surfaces. Bilayer exciton condensates are counterflow superfluids with unusual electrical properties,[4,7–11] which have so far been studied experimentally mainly in the quantum Hall regime. In this Rapid Communication we point out that superfluidity is likely to persist to remarkably high temperatures in graphene-based bilayers. Graphene is a particularly attractive candidate for room-temperature bilayer exciton condensation because it is atomically two dimensional, because it is a gapless semiconductor, and because its two-dimensional massless Dirac-band structure implies nearly perfect particle-hole symmetry and stiff phase order.

We consider a system with two graphene layers embedded in a dielectric media and gated above and below, as illustrated schematically in Fig. 1. Each layer has two Dirac-cone bands centered at inequivalent points in its Brillouin zone. The top and bottom gates can be used to control the electric fields E_{ext} both above and below the bilayer. When the two fields are equal the bilayer is neutral, but charge is transferred from one layer to the other. The Fermi level lies in the graphene conduction band of one layer (the n-type layer) and in the valence band of the other layer (the p-type layer). The particle-hole symmetry of the Dirac equation ensures perfect nesting[12] between the electron Fermi spheres in the n-type layer and its hole counterparts in the opposite layer, thereby driving the Cooper instability. The condensed state establishes spontaneous long-range coherence between the two graphene layers.

Our main interest here is in providing an estimate of the maximum possible Kosterlitz-Thouless (KT) temperature T_{KT} of these two-dimensional counterflow superfluids.[4] We use a two-band model[13] in which the occupied valence band of the n-type layer and the empty conduction band of the p-type layer are neglected. Our T_{KT} estimate is constructed from mean-field (Hartree-Fock) theory calculations[14] of the temperature-dependent phase stiffness of the ordered state.

Our main result is the normal to superfluid phase boundary depicted in Fig. 2. The KT temperature is plotted as a function of the separation between the layers d and the electric field E_{ext} outside the bilayer. We estimate that superfluidity can survive at room temperature under favorable experimental conditions. The nonmonotonic dependence of T_{KT} on d at fixed E_{ext} follows from a competition between the increasing carrier density and the decreasing strength of interlayer electron-hole interactions with increasing d. At small d the phase stiffness is limited by the carrier concentration, which increases with d. At large d, the KT temperature is limited by the same fermion-entropy effects, which are responsible for the Bardeen-Cooper-Schrieffer (BCS) critical temperature of weak-coupling superconductors.

II. TWO-BAND MEAN-FIELD THEORY

In the band eigenstate representation, our band Hamiltonian is $\mathcal{H}^{\text{B}}=-\Sigma_{\boldsymbol{k},\sigma',\sigma}c^{\dagger}_{\boldsymbol{k},\sigma'}\epsilon_k\tau^z_{\sigma'\sigma}c_{\boldsymbol{k},\sigma}$, where $\epsilon_k=V_g/2-\hbar vk$, v is the band quasiparticle velocity, $\boldsymbol{\tau}$ is a Pauli-matrix vector which acts on the *which layer* pseudospin, and $V_g=eE_{\text{ext}}d$ is the gate-induced potential difference between the two layers.

Spontaneous interlayer coherence is induced by interlayer Coulomb interactions. In the mean-field description the in-

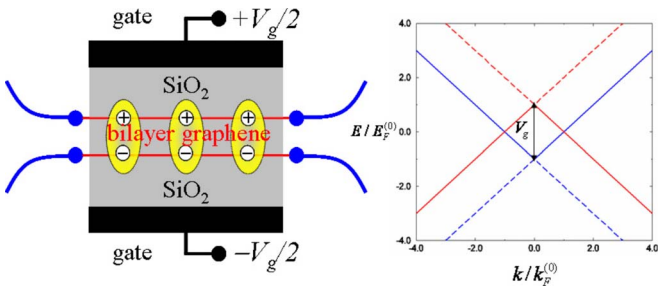

FIG. 1. (Color online) Left: Schematic of a graphene bilayer exciton condensate channel in which two single-layer graphene sheets are separated by a dielectric (SiO_2 in this illustration) barrier. We predict that electron and hole carriers induced by external gates will form a high-temperature exciton condensate. Right: The two-band model in which the two remote bands indicated by dashed lines are neglected.

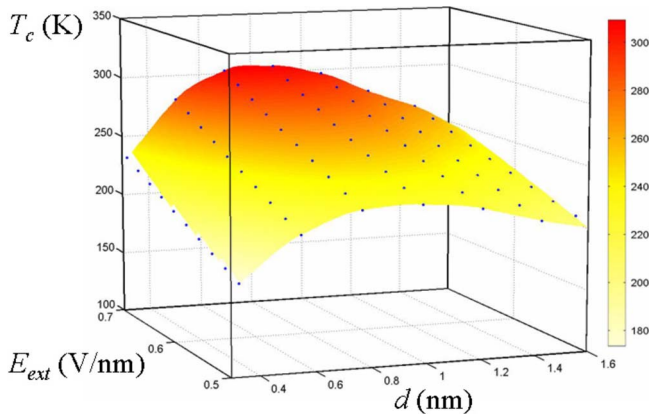

FIG. 2. (Color online) Normal to superfluid phase diagram showing the dependence of the critical temperature T_c in K on the distance between layers d in nm and external bias electric field E_{ext} in V/nm.

terlayer interaction reorganizes the low-energy fermionic degrees of freedom into quasiparticles, which are phase-coherent linear combinations of the single-layer states. The mean-field theory Hamiltonian can be written in the following form:[15]

$$\mathcal{H}^{\mathrm{MF}} = -\sum_{k,\sigma',\sigma} c^{\dagger}_{k,\sigma'}(\Delta^0_k \delta_{\sigma',\sigma} + \boldsymbol{\Delta}_k \cdot \boldsymbol{\tau}_{\sigma',\sigma}) c_{k,\sigma}. \tag{1}$$

Because of the model's particle-hole symmetry, Δ^0 vanishes. The pseudospin effective field $\boldsymbol{\Delta}_k$ in Eq. (1) solves the following self-consistent equation:

$$\Delta^z_k = \epsilon_k + \frac{1}{2A}\sum_p \left[V^{(\mathrm{S})}_{k,p} - \frac{2\pi e^2}{\epsilon} gd \right][1 + f_d(\Delta_p) n_z(\boldsymbol{\Delta}_p)],$$

$$\boldsymbol{\Delta}^{\perp}_k = \frac{1}{2A}\sum_p V^{(\mathrm{D})}_{k,p} f_d(\Delta_p) \boldsymbol{n}^{\perp}(\boldsymbol{\Delta}_p), \tag{2}$$

where A is the area of a graphene layer, $\boldsymbol{\Delta}^{\perp}_k = (\Delta^x_k, \Delta^y_k)$, $\boldsymbol{n}$ is a unit vector parallel to $\boldsymbol{\Delta}_k$, $g=4$ accounts for the spin and valley degeneracy, and $f_d(x) = \tanh(x/2T)$ is the difference between the occupation numbers of the negative-energy and positive-energy quasiparticles. The Coulomb matrix element of the intralayer interactions in the eigenstate basis is

$$V^{(\mathrm{S})}_{k,p} = \frac{1}{\epsilon}\frac{2\pi e^2}{|\boldsymbol{k}-\boldsymbol{p}|}\frac{1+\cos(\phi_k - \phi_p)}{2}, \tag{3}$$

where ϵ is the dielectric constant characterizing the embedding media and $\phi_k = \tan^{-1}(k_y/k_x)$. The corresponding matrix element of the interlayer interaction is $V^{(\mathrm{D})}_{k,p} = V^{(\mathrm{S})}_{k,p} \exp(-|\boldsymbol{k}-\boldsymbol{p}|d)$. All energies are measured relative to the Dirac-point chemical potential of the balanced bilayer.[16] Note that each spin and valley pairs independently and that electron-hole condensation is indifferent to spin-valley space rotation in either layer.

The interaction strength in a graphene monolayer is usually characterized by the dimensionless effective fine-structure constant $\alpha = e^2/\epsilon\hbar v$. This constant naturally appears in Eq. (2) if energies and momentum are expressed in units

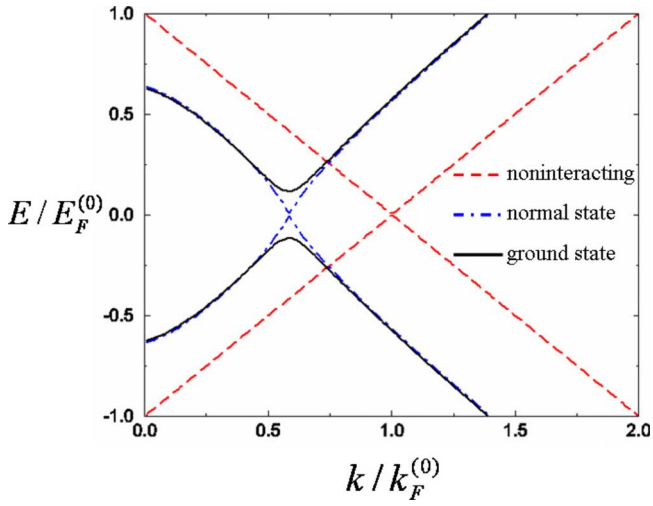

FIG. 3. (Color online) Mean-field theory energy bands for $\alpha = 1$, $T=0$, and $k_F^{(0)}d = 1$. ($E_F^{(0)} = \hbar v k_F^{(0)} = V_g/2$.) Note that $k_F < k_F^{(0)}$ because E_{ext} is screened.

of $\hbar v k_F^{(0)}$ and $k_F^{(0)}$, respectively. Here $\hbar v k_F^{(0)} = V_g/2$ is the band Hamiltonian Fermi momentum. The strength of the interlayer interaction is determined by α and by $k_F^{(0)}d$.

Interestingly, the self-consistent Eq. (2) admits solutions with nonzero chirality J of the gap function $\boldsymbol{\Delta}^{\perp}$: $\boldsymbol{\Delta}^{\perp}_k = \Delta^{\perp}_k[\cos(J\phi_k), \sin(J\phi_k)]$. However, the critical temperature of a state with nonzero chirality is higher than that of the corresponding T_c of the zero chirality ground state, so these solutions are unlikely to be physically relevant. We focus on the $J=0$ solutions hereafter.

In the normal state, there is no interlayer coherence so $\boldsymbol{\Delta}^{\perp}$ vanishes. The intralayer Hartree-Fock potential then follows from self-consistent solution for Δ^z. The main effects of electron-electron interactions in this case are to increase the bare quasiparticle velocity[17] and to screen the external bias voltage. Screening reduces the amount of charge transfer and therefore reduces the normal-state Fermi momentum. As illustrated in Fig. 3 the energy bands change qualitatively in the condensed state because interlayer interactions induce coherence between the two layers and open an energy gap.

III. LINEARIZED GAP EQUATION

The mean-field theory phase boundary between the normal phase and superfluid phase is obtained by solving the linearized gap equation,

$$\boldsymbol{n}^{\perp}(\boldsymbol{\Delta}_k) = \frac{1}{A}\sum_p M_{k,p} \boldsymbol{n}^{\perp}(\boldsymbol{\Delta}_p), \tag{4}$$

obtained by linearizing Eq. (2) with respect to $\boldsymbol{\Delta}^{\perp}$. The kernel

$$M_{k,p} = \frac{1}{2\Delta^z_k} V^{(\mathrm{D})}_{k,p} f_d(\Delta^z_p) \tag{5}$$

of the linearized gap equation is obtained by solving the self-consistent equation for Δ^z in the normal phase. The normal phase is stable provided that all the eigenvalues of M are

smaller than one. By numerically evaluating M for various interlayer distances and external fields, we find the mean-field phase diagram $T_c^{\mathrm{MF}}(d,E_{\mathrm{ext}})$ (not shown).

IV. PHASE STIFFNESS

In two-dimensional superfluids, the critical temperature is often substantially overestimated by mean-field theory and is ultimately limited by entropically driven vortex and antivortex proliferation at the KT temperature

$$T_{\mathrm{KT}} = \frac{\pi}{2}\rho_s(T_{\mathrm{KT}}). \tag{6}$$

We estimate T_{KT} by using mean-field theory to calculate the phase stiffness (superfluid density) $\rho_s(T)$. In parabolic band systems, this procedure yields reasonable estimates of T_{KT} in both BCS and Bose-Einstein condensation (BEC) limits.

The phase stiffness is most easily calculated by evaluating the counterflow current $\boldsymbol{j_Q}=(e/\hbar)\rho_s\boldsymbol{Q}$ at small exciton momentum $\boldsymbol{Q}$. Put formally, we evaluate the expectation value of the counterflow current operator,

$$j_{\boldsymbol{Q}}^{\mathrm{D}} = -\frac{ev}{A}\sum_{\boldsymbol{k}\sigma}\cos\,\phi_{\boldsymbol{k}}\langle c_{\boldsymbol{k},\sigma}^{\dagger}c_{\boldsymbol{k},\sigma}\rangle, \tag{7}$$

with the density matrix defined by the mean-field Hamiltonian

$$\mathcal{H}^{\mathrm{MF}} = \mathcal{H}^{\mathrm{B}} + \sum_{\boldsymbol{k}}(\Delta_{\boldsymbol{kQ}}^{\perp}c_{\boldsymbol{k}+\boldsymbol{Q}/2,\uparrow}^{\dagger}c_{\boldsymbol{k}-\boldsymbol{Q}/2,\downarrow} + \mathrm{H.c.}), \tag{8}$$

where $\Delta_{\boldsymbol{kQ}}^{\perp}$ is the finite momenta pairing potential.

Placing $\boldsymbol{Q}$ along $\hat{\boldsymbol{x}}$, we find that $\Delta_{\boldsymbol{k}}^{0}\rightarrow\frac{1}{2}\hbar Qv\cos\phi_k$ and that

$$j_{\boldsymbol{Q}}^{\mathrm{D}} = \frac{evQ}{4\pi}\int dk\left[\hbar vk\frac{\partial f(\Delta_k)}{\partial\Delta_k} - \frac{1}{2}f_d(\Delta_k)\hat{n}_z(\Delta_k)\right] \tag{9}$$

($\Delta_k^z=\epsilon_k$). This expression for $j_{\boldsymbol{Q}}^{\mathrm{D}}$ has an ultraviolet divergence and fails to vanish in the normal state ($\Delta^{\perp}\rightarrow 0$). Both properties are pathologies of the Dirac model. When the two Fermi circles are shifted in opposite directions at finite Q, they are asymmetric with respect to the momentum-space origin. As a consequence an ultraviolet cutoff at some momentum magnitude yields a finite counterflow current. This current would vanish if the same calculation was performed using a microscopic model with integrations over the full Brillouin zone. As long as $\Delta^{\perp}$ is small compared to the graphene's π bandwidth (a condition that is very easily satisfied), the anomalous ultraviolet contribution to $\rho_s(T)$ is identical in the normal and in the condensed states. It follows that the physical counterflow current is related to the Dirac model counterflow current (j^{D}) by $j_{\boldsymbol{Q}}=j_{\boldsymbol{Q}}^{\mathrm{D}}(\Delta)-j_{\boldsymbol{Q}}^{\mathrm{D}}(\Delta^{\perp}=0)$. Following this prescription, we conclude that the last term in Eq. (9) can be neglected and find that

$$\rho_s(T) \approx \frac{v^2\hbar^2}{16\pi T}\int kdk\left[\mathrm{sech}^2\left(\frac{\epsilon_k}{2T}\right) - \mathrm{sech}^2\left(\frac{\Delta_k}{2T}\right)\right]. \tag{10}$$

Note that the zero-temperature phase stiffness,

$$\rho_s(T=0) \approx \frac{E_F}{4\pi} \tag{11}$$

is purely a normal-state property just as in BCS theory. Indeed an identical result is obtained in the BCS theory of a parabolic band system when ρ_s is expressed in terms of the Fermi energy.

An alternative approach for estimating $\rho_s(T)$, which also accounts for the intralayer interactions, is to evaluate the density matrix in Eq. (7) using the self-consistent mean-field equations with finite pairing momentum. As explained above, the physical counterflow current is obtained by subtracting $j_{\boldsymbol{Q}}^{\mathrm{D}}(\Delta^{\perp}=0)$ from $j_{\boldsymbol{Q}}^{\mathrm{D}}$. The KT temperatures, which follow from this procedure and from Eq. (6), are depicted in Fig. 2. Since $\rho_s(T)$ is a decreasing function of d, it follows from Eqs. (6) and (11) that $T_{\mathrm{KT}}\leq E_F/8$. In our calculations we find that this inequality approaches an equality when k_Fd is small. Consequently, the increase in T_{KT} with d at small d in Fig. 2 simply follows the increase in $E_F\sim eE_{\mathrm{ext}}d/2$.

V. DISCUSSION

The high-transition temperatures we predict deserve comment. They are larger than those of typical superconductors because condensation is driven by Coulomb interactions over the full bandwidth, rather than by phonon-mediated interactions between quasiparticles in a narrow shell around the Fermi surface. In this sense exciton condensation is more akin to ferromagnetism, which is also driven by Coulomb interactions and can survive to very high temperatures. The temperatures at which exciton condensation can be achieved in graphene bilayers are immensely higher than those which might be possible in semiconductor bilayers because more carriers can be induced by external electric fields when the semiconductor has no gap, because the Fermi energy increases more rapidly with carrier density for Dirac bands than for parabolic bands, and because graphene layers are atomically thin, eliminating the layer thickness effects that substantially weaken Coulomb interaction in semiconductor quantum well bilayers. The numerical estimates reported in Fig. 2 were obtained using a coupling constant appropriate for a SiO_2 dielectric. The optimal dielectric for high-exciton condensation temperatures should have a high dielectric breakdown field and a low dielectric constant, suggesting that a suitable wide-gap material is likely the optimal choice.

Screening and other beyond mean-field induced-interaction effects are difficult to describe. In the case of weakly interacting atomic gases, induced-interaction effects can[18] either increase or decrease T_c, depending on the number of fermion flavors g. For the present Coulomb interaction case, a static Thomas-Fermi screening approximation with normal-state screening wave vectors reduces interaction strengths very substantially when spin and valley degeneracies ($g=4$) are included. Mean-field theory critical temperatures are reduced by a factor of $\sim e^g$ at small d in this approximation and by a larger factor at large d. On the other hand, when the screening wave vectors are evaluated in the condensed state, there is little influence on T_{KT} at small k_Fd both because the large gap weakens screening and because

T_{KT} is proportional to the Fermi energy and not to the interaction strength in this limit. All this leads us to suspect that at low temperatures, there is a first-order phase transition as a function of layer separation d between condensed and electron-hole plasma states, similar to the transitions studied experimentally[19] in quantum Hall exciton condensates and theoretically[20] in parabolic band bilayers.

Because of spin and valley degrees of freedom, the exciton pairing we describe in this work is SU(4) symmetric; crudely speaking the system has four identical superfluids simultaneously. We therefore anticipate interesting consequences of slightly unequal electron and hole densities, similar to anticipated effects associated with the spin degree of freedom in normal exciton condensates.[21,22] Because of this sensitivity, front and back gates, which can control the electric fields on opposite sides of the bilayer independently, are highly desirable in experimental searches for graphene bilayer exciton condensation.

Our finding that $T_{KT} \sim 0.1 E_F$ in the limit of strong interactions between conduction-band electrons and valence-band holes is partially supported by experimental studies[23] of fermionic cold atoms in the strong-interaction unitary limit. It implies that T_{KT} should approach room temperature when E_F is larger than ~ 0.3eV (n larger than $\sim 10^{13}$ cm^2) and d is smaller than ~ 2 nm. Experimental detection of spontaneous coherence through one of its characteristic transport anomalies[4] will be necessary to construct a quantitatively reliable phase diagram.

ACKNOWLEDGMENTS

This work was supported by the Welch Foundation, by the Army Research Office, by the NRI SWAN Center, and by the National Science Foundation under Grant No. DMR-0606489. A.H.M. acknowledges helpful discussions with Rembert Duine, Koos Gubbels, and Henk Stoof.

[1] J. M. Blatt, K. W. Böer, and W. Brandt, Phys. Rev. **126**, 1691 (1962).

[2] L. V. Keldysh and A. N. Kozlov, Sov. Phys. JETP **27**, 521 (1968).

[3] I. B. Spielman, J. P. Eisenstein, L. N. Pfeiffer, and K. W. West, Phys. Rev. Lett. **84**, 5808 (2000); **87**, 036803 (2001).

[4] J. P. Eisenstein and A. H. MacDonald, Nature (London) **432**, 691 (2004), and work cited therein.

[5] L. V. Butov, J. Phys.: Condens. Matter **19**, 295202 (2007).

[6] See, for example, J. Kasprzak, M. Richard, S. Kundermann, A. Baas, P. Jeambrun, J. M. J. Keeling, F. M. Marchetti, M. H. Szymńska, R. André, J. L. Staehli, V. Savona, P. B. Littlewood, B. Deveaud, and Le Si Dang, Nature (London) **443**, 409 (2006); D. Sarchi and V. Savona, Solid State Commun. **144**, 371 (2007); Y. E. Lozovik and A. G. Semenov, JETP Lett. **86**, 28 (2007), and work cited therein.

[7] J. A. Seamons, D. R. Tibbetts, J. L. Reno, and M. P. Lilly, Appl. Phys. Lett. **90**, 052103 (2007).

[8] K. Das Gupta, M. Thangaraj, A. F. Croxall, H. E. Beere, C. A. Nicoll, D. A. Ritchie, and M. Pepper, Physica E (Amsterdam) **40**, 1693 (2008).

[9] K. Moon, H. Mori, K. Yang, S. M. Girvin, A. H. MacDonald, L. Zheng, D. Yoshioka, and S.-C. Zhang, Phys. Rev. B **51**, 5138 (1995).

[10] A. V. Balatsky, Y. N. Joglekar, and P. B. Littlewood, Phys. Rev. Lett. **93**, 266801 (2004).

[11] J.-J. Su and A. H. MacDonald, arXiv:0801.3694 (unpublished).

[12] The nesting condition requires only that the Fermi surfaces be identical in area and shape and not that the two layers have aligned honeycomb lattices and hence aligned Brillouin zones. Global wave vector mismatches can be removed by gauge transformations. When weak inter-valley electron-electron scattering processes are included only simultaneous momentum shifts of both valleys in a layer are allowed. In this case relative rotations of the two layers will have a small influence on details of the paired state. Relative rotations will also help to reduce the amplitude of bare interlayer tunneling process which weaken transport anomalies as discussed in Ref. 11. For misaligned layers, bare tunneling could possibly be weak enough to produce interesting transport anomalies even for vertical transport between epilayers similar to those discussed by J. Hass, F. Varchon, J. E. Millan-Otoya, M. Sprinkle, N. Sharma, W. A. de Heer, C. Berger, P. N. First, L. Magaud, and E. H. Conrad, Phys. Rev. Lett. **100**, 125504 (2008).

[13] In separate calculations not described here we found that coherence between the two remote bands has little effect for $k_F d > 1$ and that will act to raise the KT temperature for $k_F d < 1$.

[14] In parabolic band systems this procedure provides a good estimate of the critical temperature in both the weak-coupling BCS and the strong-coupling BEC limits. Note, however, that because graphene is a gapless semiconductor, it does not have a simple BEC strong-coupling limit.

[15] Hongki Min, G. Borghi, M. Polini, and A. H. MacDonald, Phys. Rev. B **77**, 041407(R) (2008).

[16] The unit contribution to the right-most square-bracket factor in Eq. (2) for $\Delta_{\mathbf{k}}^{z}$ is due to exchange interactions with the full valence band of the n-type layer.

[17] Y. Barlas, T. Pereg-Barnea, M. Polini, R. Asgari, and A. H. MacDonald, Phys. Rev. Lett. **98**, 236601 (2007).

[18] H. Heiselberg, C. J. Pethick, H. Smith, and L. Viverit, Phys. Rev. Lett. **85**, 2418 (2000).

[19] A. R. Champagne, J. P. Eisenstein, L. N. Pfeiffer, and K. W. West, Phys. Rev. Lett. **100**, 096801 (2008).

[20] S. De Palo, F. Rapisarda, and G. Senatore, Phys. Rev. Lett. **88**, 206401 (2002).

[21] E. Bascones, A. A. Burkov, and A. H. MacDonald, Phys. Rev. Lett. **89**, 086401 (2002).

[22] M. Y. Veillette and L. Balents, Phys. Rev. B **65**, 014428 (2001).

[23] Y. Shin, C. H. Schunck, A. Schirotzek, and W. Ketterle, Nature (London) **451**, 689 (2008).